Electronic Supplementary Material (ESI) for Soft Matter.

Supporting Information for:

Ultralong cylindrical micelles precisely located with semiconductor nanorods by solvent evaporation-driven self-assembly

Xiaobo Nie[a,b], Jie Cui[a] and Wei Jiang*[a]

[a] State Key Laboratory of Polymer Physics and Chemistry, Changchun Institute of Applied Chemistry, Chinese Academy of Sciences, Changchun 130022, P. R. China

[b] University of Chinese Academy of Sciences, Beijing 100049, P. R. China

* Corresponding author. E-mail: wjiang@ciac.ac.cn

SUPPORTING DATA

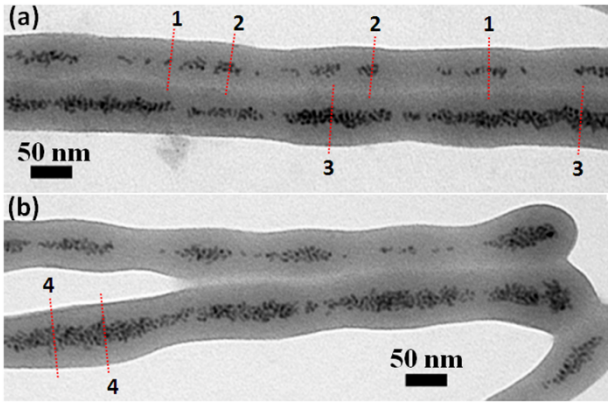

Fig. S1 (a) and (b) Bright-field TEM images showing the numbers of the PS-NRs randomly oriented in the central portions of the hybrid cylinders in the corresponding cross-sections. The red dash lines meant the cross-sections of the hybrid cylinders and the numbers nearby were the amounts of the PS-NRs in the corresponding cross-sections.

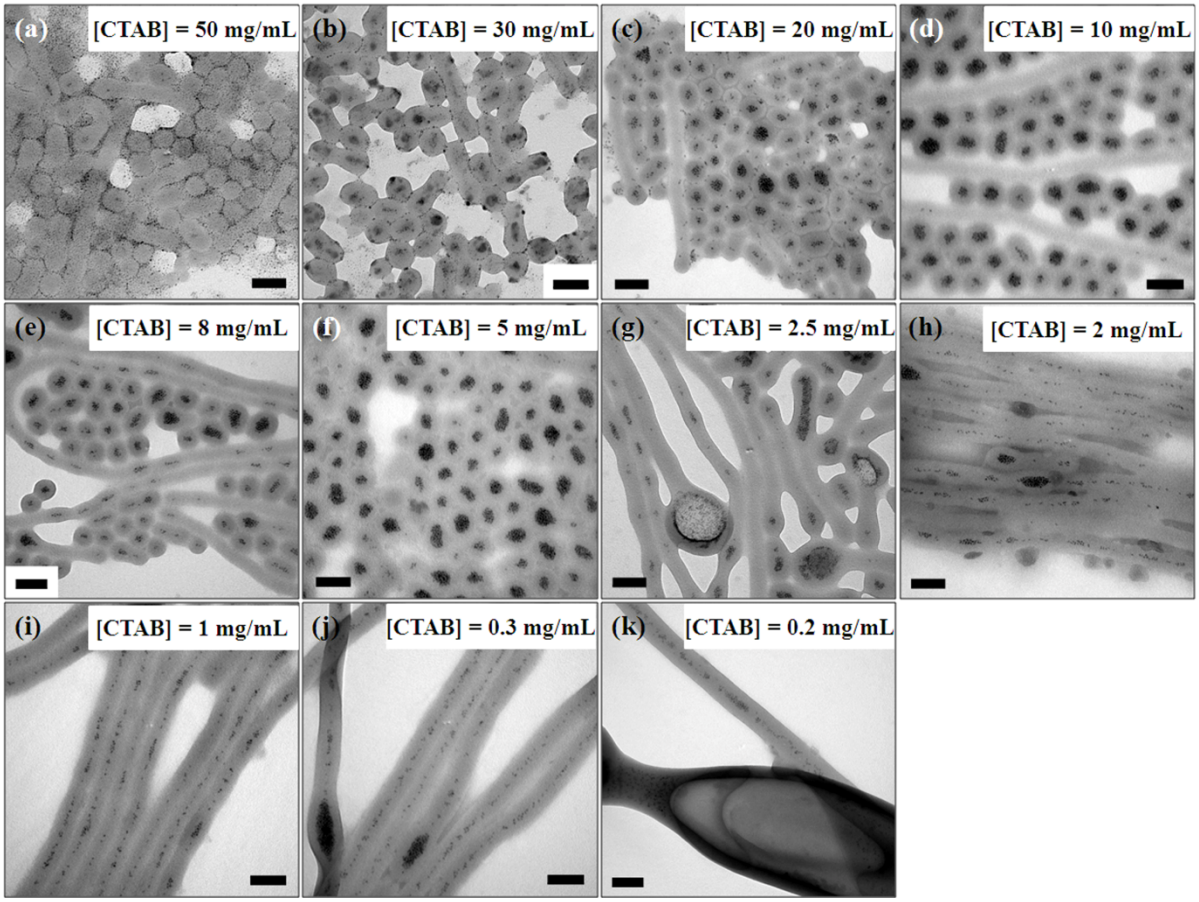

Fig. S2 (a-k) Bright-field TEM images of coassemblies formed from PS-NRs (f = 0.1) and PS_{356}-*b*-PEO_{148} in $CHCl_3$-in-H_2O emulsions (V_{CHCl_3}:V_{H_2O} = 1:5) at magnetic stirring rate of 750 rpm, but varied [CTAB] as depicted in the top right corner of the corresponding image: (a) 50 mg/mL; (b) 30 mg/mL; (c) 20 mg/mL; (d) 10 mg/mL; (e) 8 mg/mL; (f) 5 mg/mL; (g) 2.5 mg/mL; (h) 2 mg/mL; (i) 1 mg/mL; (j) 0.3 mg/mL; (k) 0.2 mg/mL. All scale bars in the TEM images are 100 nm.

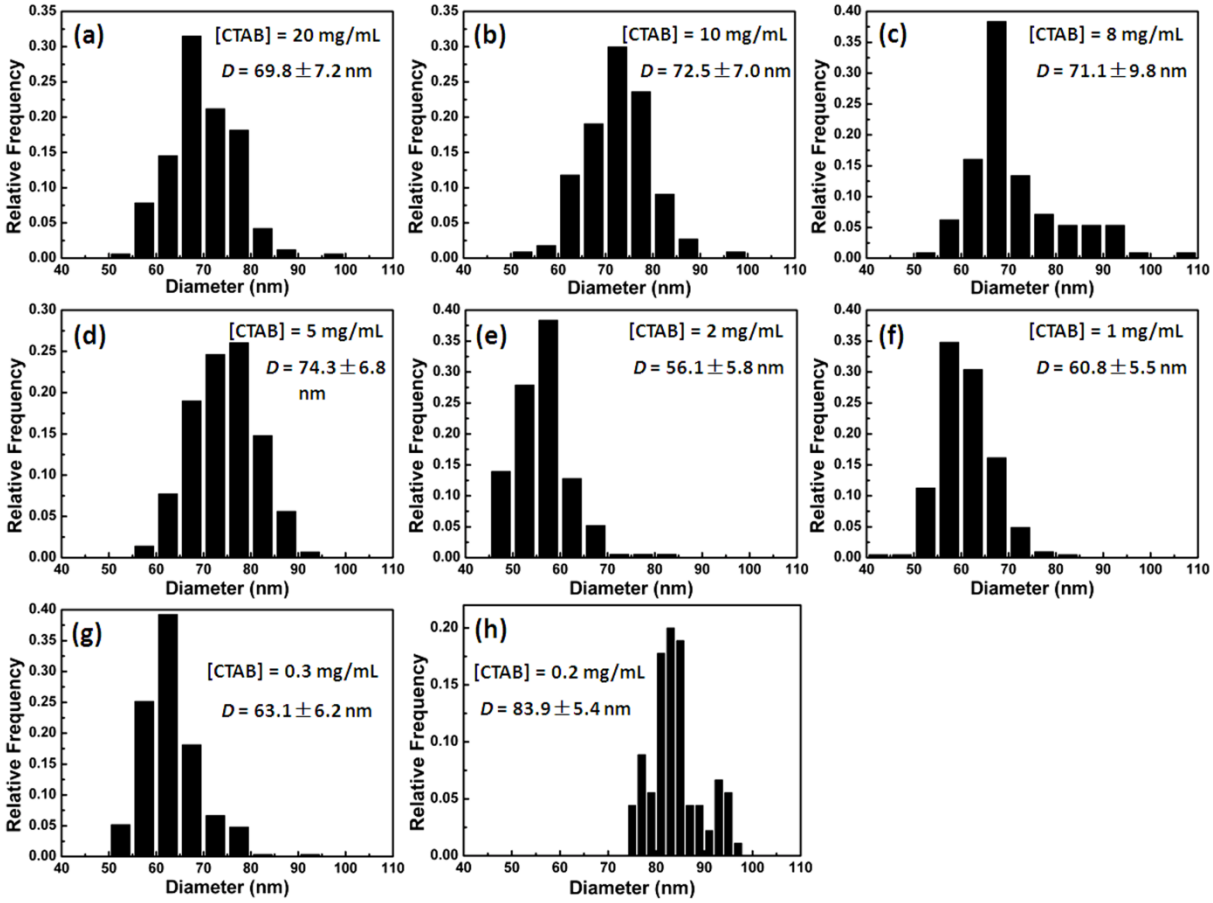

Fig. S3 Distributions of the statistic diameters of the coassemblies formed from PS-NRs (f = 0.1) and PS_{356}-*b*-PEO_{148} in $CHCl_3$-in-H_2O emulsions (V_{CHCl_3}:V_{H_2O} = 1:5) at magnetic stirring rate of 750 rpm, but varied [CTAB]: (a) [CTAB] = 20 mg/mL, D = 69.8 ± 7.2 nm; (b) [CTAB] = 10 mg/mL, D = 72.5 ± 7.0 nm; (c) [CTAB] = 8 mg/mL, D = 71.1 ± 9.8 nm; (d) [CTAB] = 5 mg/mL, D = 74.3 ± 6.8 nm; (e) [CTAB] = 2 mg/mL, D = 56.1 ± 5.8 nm; (f) [CTAB] = 1 mg/mL, D = 60.8 ± 5.5 nm; (g) [CTAB] = 0.3 mg/mL, D = 63.1 ± 6.2 nm; (h) [CTAB] = 0.2 mg/mL, D = 83.9 ± 5.4 nm.

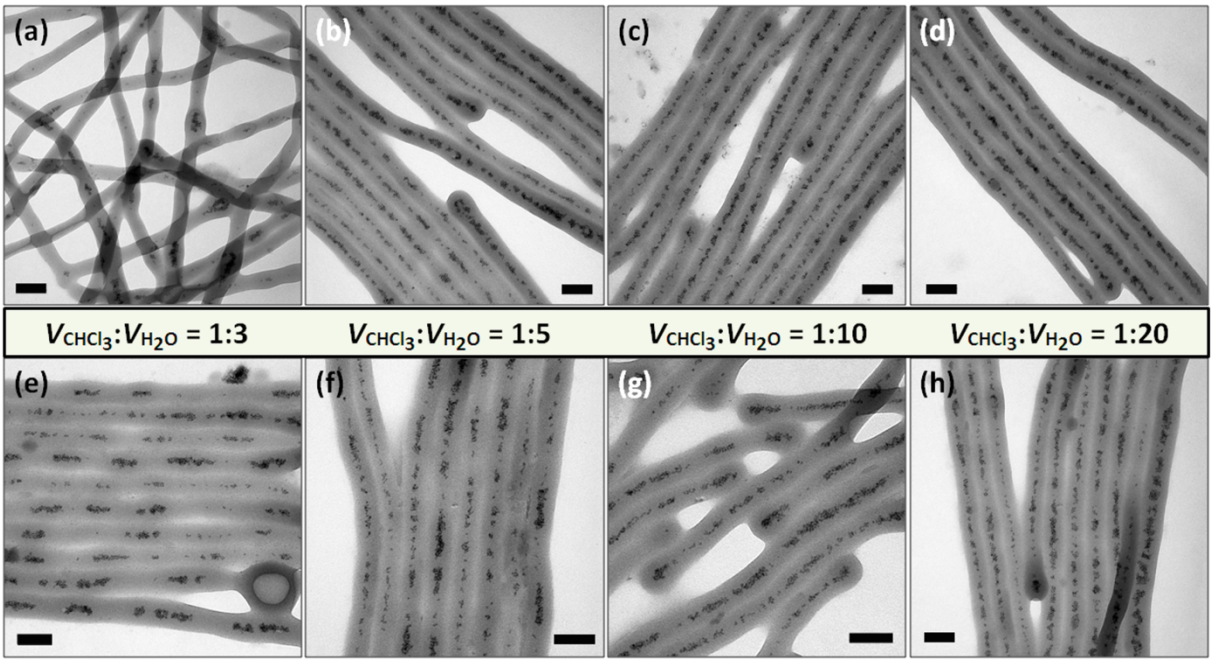

Fig. S4 (a-h) Bright-field TEM images of cylindrical micelles with PS-NRs loaded in their central cores formed from PS-NRs (f = 0.1) and PS_{356}-*b*-PEO_{148} in $CHCl_3$-in-H_2O emulsions at different V_{CHCl_3}:V_{H_2O} when [CTAB] = 1 mg/mL and magnetic stirring rate was 750 rpm. (a-d) V_{CHCl_3} = 0.2 mL, but varied V_{H_2O}; (e-h) V_{H_2O} = 1 mL, but varied V_{CHCl_3}. The V_{CHCl_3}:V_{H_2O} was set to be (a, e) 1:3, (b, f) 1:5, (c, g) 1:10 and (d, h) 1:20, respectively. All scale bars in the TEM images are 100 nm.

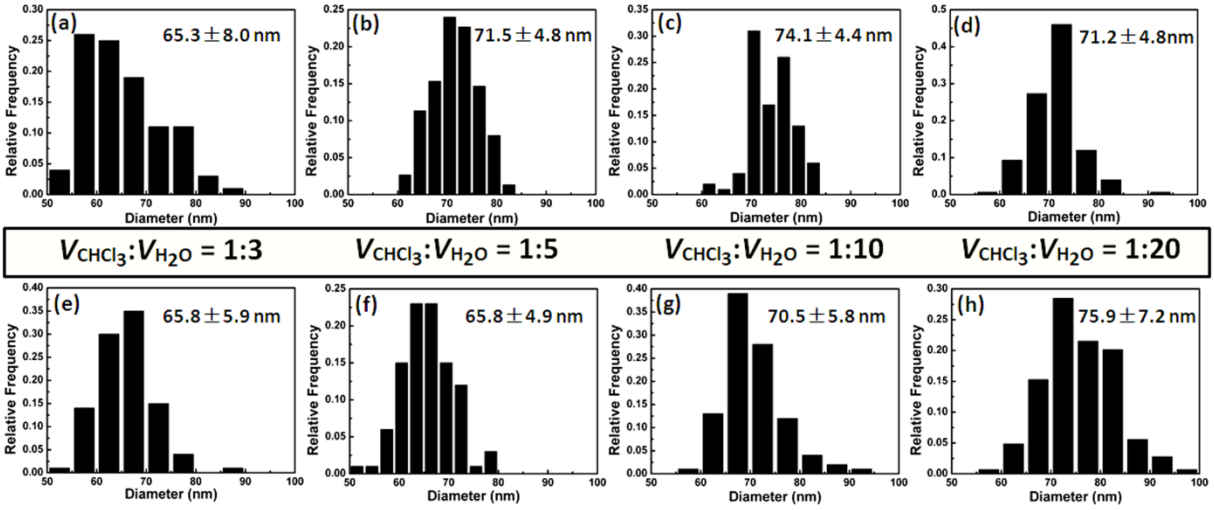

Fig. S5 (a-h) Distributions of the statistic diameters of the hybrid cylinders formed from PS-NRs (f = 0.1) and PS_{356}-*b*-PEO_{148} in $CHCl_3$-in-H_2O emulsions at different V_{CHCl_3}:V_{H_2O} when [CTAB] = 1 mg/mL and magnetic stirring rate was 750 rpm. (a-d) V_{CHCl_3} = 0.2 mL, but varied V_{H_2O}; (e-h) V_{H_2O} = 1 mL, but varied V_{CHCl_3}. The V_{CHCl_3}:V_{H_2O} was set to be (a, e) 1:3, (b, f) 1:5, (c, g) 1:10 and (d, h) 1:20, respectively.

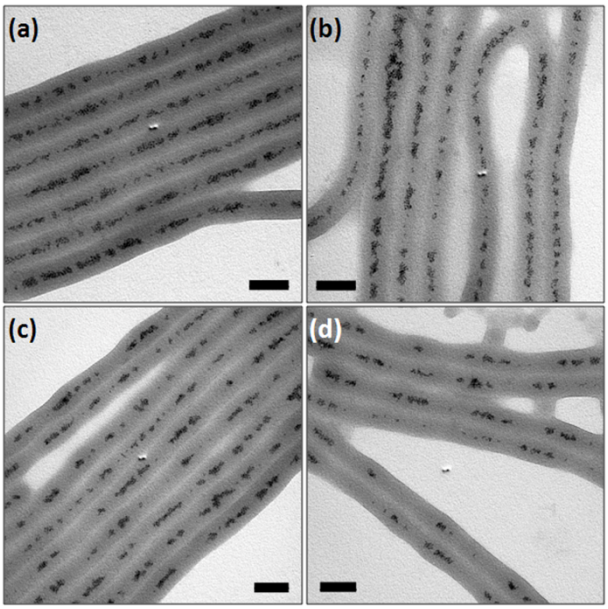

Fig. S6 (a-d) Bright-field TEM images of cylindrical micelles with PS-NRs loaded in their central cores formed from PS-NRs (f = 0.1) and PS_{356}-*b*-PEO_{148} in $CHCl_3$-in-H_2O emulsions (V_{CHCl_3}:V_{H_2O} = 1:5) in the presence of CTAB ([CTAB] = 1 mg/mL) under different magnetic stirring rate: (a) 500 rpm; (b) 750 rpm; (c) 1000 rpm; (d) 1500 rpm. All scale bars in the TEM images are 100 nm.

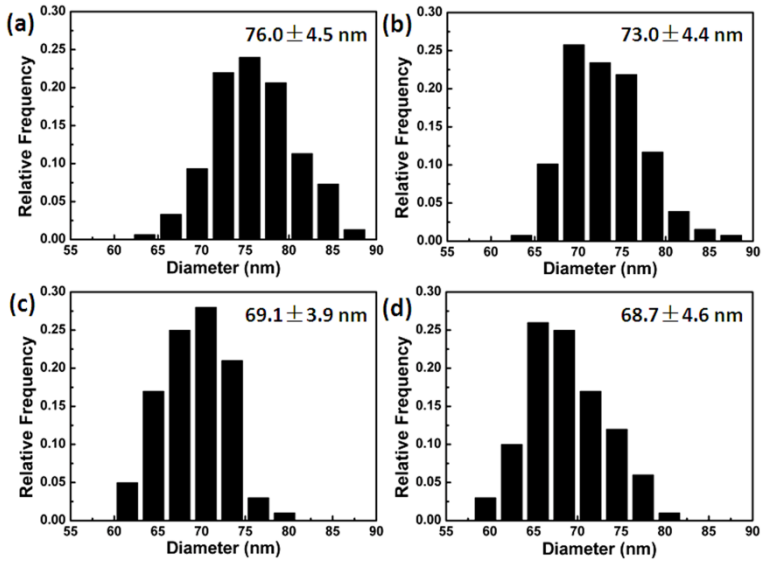

Fig. S7 (a-d) Distributions of the statistic diameters of the hybrid cylinders formed from PS-NRs (f = 0.1) and PS_{356}-*b*-PEO_{148} in $CHCl_3$-in-H_2O emulsions (V_{CHCl_3}:V_{H_2O} = 1:5) in the presence of CTAB ([CTAB] = 1 mg/mL) under different magnetic stirring rate: (a) 500 rpm; (b) 750 rpm; (c) 1000 rpm; (d) 1500 rpm.